ELSEVIER

Contents lists available at ScienceDirect

Remote Sensing of Environment

journal homepage: www.elsevier.com/locate/rse





CubeSats show persistence of bull kelp refugia amidst a regional collapse in California

Katherine C. Cavanaugh ^{a,*}, Kyle C. Cavanaugh ^a, Camille C. Pawlak ^a, Tom W. Bell ^b, Vienna R. Saccomanno ^c

- ^a University of California, Los Angeles, CA, United States of America
- b Woods Hole Oceanographic Institution, Woods Hole, MA, United States of America
- ^c The Nature Conservancy, Sacramento, CA, United States of America

ARTICLE INFO

Edited by Dr. Marie Weiss

Keywords:
CubeSat
PlanetScope
Planet Dove
Merged sensors
Fine-scale data
Coastal ecology
Disturbance ecology
Refugia

ABSTRACT

Bull kelp populations in northern California declined drastically in response to the 2014–2016 marine heatwave, sea star wasting disease, and subsequently large increases in herbivorous purple urchin populations. Despite the regional kelp forest collapse, there were small, remnant populations where bull kelp was able to survive. Moderate resolution satellites (i.e., Landsat) have been important for creating long-term, large-scale time series of bull kelp forests, however, these have been shown to underestimate or entirely exclude refugia due to their low densities and proximity to the coastline. While measurements from Unoccupied Aerial Vehicles (UAV) are spatially detailed, they are temporally limited and difficult to collect over regional scales. The development of CubeSat constellations has enabled a workaround for these tradeoffs, with global imagery available near-daily at meter-scale

We developed a method for mapping bull kelp canopy across the different sensor cohorts in the PlanetScope constellation. This required correcting surface reflectance measurements to account for differences in the spectral response functions among the sensors and leveraging the temporal frequency of PlanetScope data to increase the automation of classifying kelp canopy in imagery with increased noise. Using the PlanetScope derived kelp canopy extents, we identified locations where bull kelp refugia have persisted in northern California. We found that bull kelp refugia occupied about 2% of the total available habitat in the region and about 9.4% of the average canopy area observed prior to 2014. These areas may be critical to the success of kelp forest reestablishment in northern California, which increases their importance for ongoing monitoring, conservation, and restoration efforts.

1. Introduction

Climate change is reshaping global biodiversity by altering abiotic conditions and biological interactions (Rosenzweig et al., 2008). The cumulative effects of contemporary climatic trends and local disturbances are exceeding the adaptive capacity and environmental tolerance of many organisms (Blowes et al., 2019), and species distributional shifts have been widely observed (Chen et al., 2011). There is also evidence that species can retreat to or persist in refuge areas that provide protection against environmental stressors, particularly when the landscape is heterogeneous (Cacciapaglia and van Woesik, 2015; Verdura et al., 2021). Here, subpopulations are likely to experience microclimates that are decoupled from regional climate variability or ecological

disturbance (Andrew and Warrener, 2017; Dobrowski, 2011). However, detecting the existence of these refugia remains challenging, as it requires observations that are sufficiently fine-scaled for target species (i. e., <1 km; Ashcroft, 2010; Kavousi and Keppel, 2018; Keppel et al., 2012).

Northern California bull kelp (*Nereocystis luetkeana*) forests constitute an example of an ecosystem that is increasingly vulnerable to climate variability. A large marine heatwave persisted along the Pacific coast of North America from 2014 to 2016, resulting in widespread temperature anomalies of up to 2.5 °C (Bond et al., 2015; Oliver et al., 2018). The heatwave coincided with mass mortality of sea star species (Harvell et al., 2019), which greatly reduced urchin predation by the sunflower sea star (*Pycnopodia helianthoides*). The combined effects of

E-mail address: kateccavanaugh@gmail.com (K.C. Cavanaugh).

^{*} Corresponding author.

the heatwave and increased grazing pressure precipitated a regional ecosystem shift from bull kelp forests to urchin barrens, resulting in deforested clearings ranging from small, meter-scale gaps to the complete denudation of entire forests across hundreds of kilometers (Rogers-Bennett and Catton, 2019). Despite the presence of expansive urchin barrens, certain sections of coastline have continued to support bull kelp populations throughout northern California (Saccomanno et al., 2022).

Bull kelp is a canopy-forming species, and the floating biomass on the water surface has been successfully quantified using aerial and satellite imagery (Finger et al., 2021; Hamilton et al., 2020; McPherson et al., 2021; Rogers-Bennett and Catton, 2019; Saccomanno et al., 2022; Schroeder et al., 2019). However, the quantification of refugia has been difficult to achieve, as the remnant populations in northern California occur in small and isolated patches that vary in density depending on the number and proximity of individuals (i.e., a single individual to a continuous forest spanning over a kilometer; Saccomanno et al., 2022). Previous work has shown that scale is important for accurately describing the existence and location of refugia, and that existing methods manifest tradeoffs between spatial, temporal, and spectral resolutions (Finger et al., 2021; Saccomanno et al., 2022).

For example, the California Department of Fish and Wildlife (CDFW) has produced annual, high resolution (2 m) statewide maps of kelp canopy from aerial surveys that date back to 1989 (Veisze et al., 1999). These maps were used to reveal the scale (> 300 km of coastline), magnitude (> 90%), and timing (within one year) of the northern California bull kelp declines, and they provided evidence that some populations were able to persist throughout the multiyear heatwave event (Rogers-Bennett and Catton, 2019). However, the last successful surveys were completed in 2016, and so they cannot be used to monitor trends in refugia or recovery following the heatwave. More recent work (e.g., Saccomanno et al., 2022) partially filled this gap with UAV equipped with RGB sensors, which were used to survey 36 non-contiguous priority sites dispersed across 90 km of affected coastline in 2019 and 2020. At 3 cm resolution, these data successfully elucidated the location of relict kelp populations within surveyed areas. However, regional UAV data collection was not cost or time effective, and classification of emergent canopy from RGB-based UAV imagery required extensive manual input. Current methods rely on thresholding vegetation indices to distinguish kelp from water (Cavanaugh et al., 2021a), and high levels of spectral variability necessitated manual threshold selection and additional editing (Saccomanno et al., 2022).

Moderate resolution satellite sensors, such as the Landsat Enhanced Thematic Mapper Plus (ETM+), Operational Land Imager (OLI), and Operational Land Imager 2 (OLI-2), provide a continuous and spatially comprehensive time series of bull kelp refugia habitat in northern California. Progress in the automation of kelp canopy detection from these data (e.g., Bell et al., 2020) includes using a binary decision tree to classify Landsat pixels that contain canopy and subsequently modeling the pixels as a combination of kelp canopy and seawater using Multiple Endmember Spectral Mixture Analysis (MESMA) to estimate fractional kelp canopy cover at a 30 m pixel scale. This method has been successfully applied to capture the abrupt ecosystem shift in northern California (McPherson et al., 2021), but the moderate resolution (30 m) was not sufficient for identifying the presence or amount of refugia that were able to persist during and after the 2014 to 2016 marine heatwave (Finger et al., 2021). These data often failed to capture microclimatic habitats that were smaller than the coverage of a single Landsat pixel (900 m²), which could potentially provide important refugia (Asner et al., 2022).

The development of CubeSat constellations has enabled a work-around for these tradeoffs, as the integration of data from multiple satellites collectively achieves higher frequency data sampling, with the ability to acquire global coverage at high spatial resolution. Planet is one of the most recognized CubeSat constellation operators, and their PlanetScope constellation contains nearly 130 active satellites. The PlanetScope CubeSats provide daily observations at 3 m resolution for

many global areas (Roy et al., 2021), and so they show great potential for monitoring fine-scale ecological dynamics (e.g., flowering events) across multiple years, at large spatial scales, and in heterogeneous landscapes (Dixon et al., 2021; Zeng et al., 2020). However, considerable geolocation inaccuracy and radiometric inconsistency between satellites and sensors remain as major challenges to the general applicability of the PlanetScope constellation for measuring environmental dynamics (Frazier and Hemingway, 2021; Leach et al., 2019). While PlanetScope data have been successfully used to detect other species of floating macroalgae (*Macrocystis pyrifera*), these methods were not automated and required manual delineation of over 75 images (Elsmore et al., 2022).

In this study, we develop and validate a model for deriving bull kelp canopy from a time series of PlanetScope CubeSat data. The PlanetScope constellation offers the high spatial (3 m) and temporal (near daily) means for mapping bull kelp refugia, and the first image collections coincide with the last statewide aerial survey conducted by CDFW in 2016. The model uses spectral features to predict bull kelp presence, and we apply it to derive annual maps of canopy coverage in northern California from 2016 to 2021.

2. Methods

2.1. Study region

Bull kelp is distributed in the northeast Pacific from San Luis Obispo County in California to Unimak Island in the eastern Aleutians (Abbott and Hollenberg, 1992; Miller and Estes, 1989). Our study area included the Sonoma and Mendocino County coastlines in northern California, extending approximately 215 km from north to south (Fig. 1). This region was historically productive and supported abundant bull kelp forests prior to the collapse that started in 2014 (Rogers-Bennett and Catton, 2019).

2.2. Image acquisition

PlanetScope 4-band Surface Reflectance data were acquired from Planet Explorer. PlanetScope images are generated from the PlanetScope satellite constellation, which contains over 130 operational 3 U Cube-Sats (10 \times 10 \times 30 cm) and provides imagery at near-daily resolution. Each sensor has an approximate ground resolution of 3 m (Planet, 2021). We acquired each pixel in the study area at ~ weekly resolution (about 5 images per month) during September and October from 2016 to 2021, resulting in a total of 2070 images. Bull kelp is an annual species and will typically undergo a full lifecycle within one calendar year. Individuals appear in the early spring, grow to canopy height by mid-summer, and reach maximum photosynthesis and canopy area in the fall before senescing in winter (Nicholson, 1970; Vadas, 1972). Imagery from September and October capture the period of peak abundance, making these months ideal for estimating refugia occupancy during and after each heatwave year. We manually digitized the coastline using Planet-Scope imagery taken at low tide and masked pixels found within the coastline boundary. We masked pixels within 10 m of the identified coastline to reduce potential misclassification from intertidal algae and terrestrial vegetation. We also masked pixels >3 km from the coastline to improve data processing times, as kelp has not historically been identified this far offshore (California Department of Fish and Wildlife, 2021).

2.3. Image processing

Merging data from the PlanetScope constellation to derive consistent kelp canopy maps through time presents various challenges, as PlanetScope sensors are not uniform across each satellite. All sensors provide four spectral bands (blue, green, red, NIR) and the same approximate ground resolution, but Planet has introduced sensor cohorts with

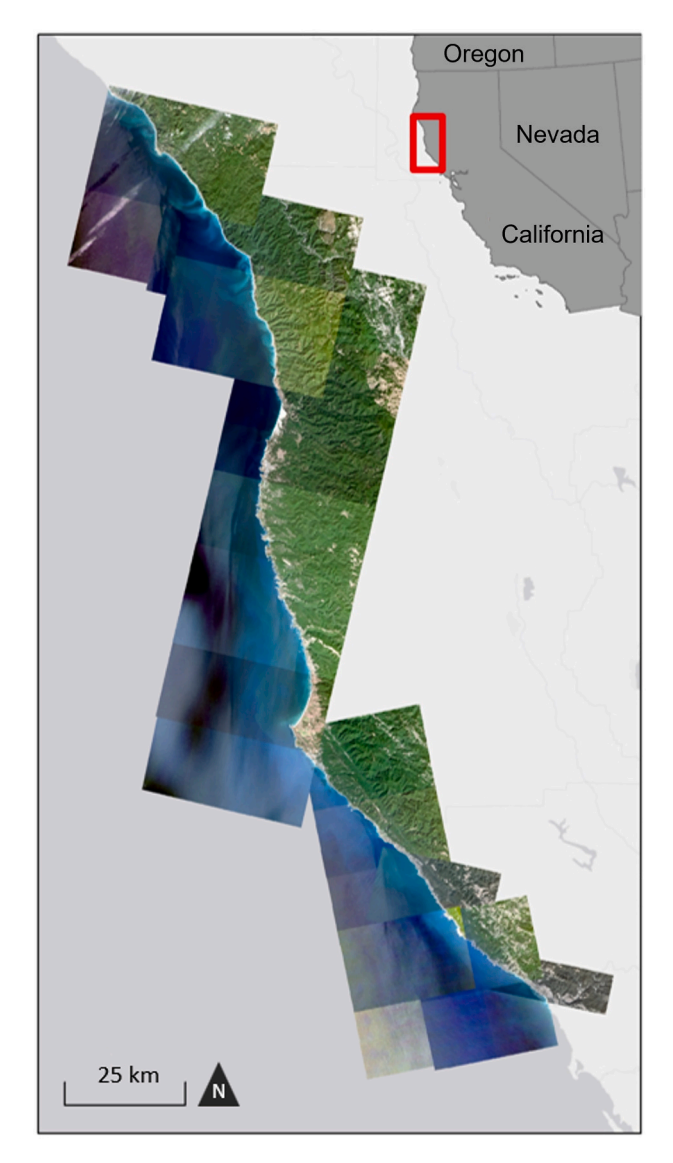


Fig. 1. Sonoma and Mendocino County regions of northern California overlaid with images from multiple PlanetScope satellites.

varying relative spectral responses and levels of noise (Planet, 2021). These cohorts are distinguished using unique 2-character satellite identification (ID) codes, which currently include 0c, 0d, 0e, 0f, 10, 11, and 20 (Planet, 2021). A number of studies have proposed methods for normalizing radiometric inconsistencies among PlanetScope data, but these often rely on image spectra from reference datasets such as Landsat 8 (Leach et al., 2019) and Sentinel-2 (Latte and Lejeune, 2020). Co-registering PlanetScope data with a reference dataset is difficult over coastal areas, as even minute differences in temporal capture may introduce significant error between pixel matchups (i.e., tides and currents). Furthermore, geolocation accuracy has been highlighted as a challenge by a number of studies that have applied these data for coastal analyses (Leach et al., 2019; Traganos et al., 2017; Wicaksono and Lazuardi, 2018).

We applied a log-residual correction (Green and Craig, 1985) to all surface reflectance images to standardize spectral reflectance values taken by different sensors in the PlanetScope constellation using the function log*Residuals* in Matlab 2020a. The log residual correction divides the spectrum of each pixel by the spectral geometric mean (mean of all bands for each pixel) and the spatial geometric mean (mean of all pixels for each band), before finally multiplying the output by the mean of all pixels in all bands (Eq. 1). This has been shown to help remove the

effects of solar irradiance, atmospheric transmittance, instrument gain, and topographic effects from image data (Ganesh et al., 2013; Green and Craig, 1985). All calculations are performed using logarithms of the data values.

$$L = |e^{input \, data-spectral \, mean-spatial \, mean+entire \, mean}|$$
 (1)

We applied the Usable Data Mask asset supplied in the PlanetScope image bundle to mask any pixels identified as unusable by Planet (i.e., sensor error, image artifacts, etc.). The Usable Data Mask 2 (UDM2) product was not used, as it was introduced by Planet in August 2018 (Planet, 2021) and was not consistently available for our imagery. We additionally masked pixels altered by sun glint and crashing waves using gray-level co-occurrence matrices (GLCM).

2.4. Kelp canopy classification

Bull kelp can be visually distinguished from water with high resolution satellite imagery (Fig. 2). Similar to terrestrial vegetation, emergent kelp canopy prominently reflects the NIR wavelength range (700 to 1000 nm). Due to the high absorbance of water in the NIR, this region of the electromagnetic spectrum is advantageous for distinguishing floating canopy from the surrounding seawater (Fig. 2; Cavanaugh et al., 2021b; Timmer et al., 2022). We manually classified a total of 93 images (~3 images per month from 2017 to 2019) covering a bull kelp bed off the coast of Ella Beach in British Columbia (48.363°, -123.757°) into two classes, 'kelp' and 'water' to capture data covered by different PlanetScope satellites, acquisition times, and view angles.

These data were used to train a two-class Naïve Bayes classifier, as previous work has shown that Naïve Bayes classifiers consistently yielded higher Kappa values than support vector machines (SVM), random forest models, and artificial neural networks when trained with PlanetScope imagery (Kranjčić and Medak, 2020). Naïve Bayes is a probabilistic supervised machine learning approach based on Bayes theorem (Park, 2016; Eq. 2).

$$P(A|B) = \frac{P(B|A)P(A)}{P(B)}$$
 (2)

Where, in the context of using corrected reflectance data from the PlanetScope constellation to predict the probability of kelp presence in each PlanetScope pixel, A refers to kelp presence and B refers to a vector of PlanetScope reflectances for each band. Therefore, P(A|B) is the conditional probability that kelp is present given the reflectance measurements from different spectral bands. The algorithm deduces a prior probability distribution from the provided training data for all bands in the 'kelp' and 'water' classes (P(A)). The prior probability distribution of data with the same predictors (i.e., an unclassified image), but an unknown class (Ahmad and Quegan, 2012; Ahmad et al., 2021). The probability distribution of the data were assumed to be normal.

We applied the resulting classifier to images taken in September and October from 2016 to 2021 to obtain the probability of pixels containing kelp in each image. We calculated monthly pixel-wise averages of probabilities and classified pixels that exceeded probabilities of 0.5 (i.e., the maximum probability for a 2-class classification) as kelp (Fig. 3). Aggregating the probability data on monthly time-steps aided in reducing error and labor-intensive manual editing due to misclassifications from radiometric and geometric issues with individual images.

2.5. Kelp canopy map validation

To validate our kelp canopy classifications, we used ordinary least squares (OLS) regressions to compare PlanetScope-derived kelp canopy area estimates to three published datasets that have classified kelp canopy in northern California between 2016 and 2021. The first



Fig. 2. A full PlanetScope scene from September 30, 2021 (A) in northern California that includes bull kelp surface canopy. Emergent canopy is visibly distinguishable in true color (B) and false color (C) composites.

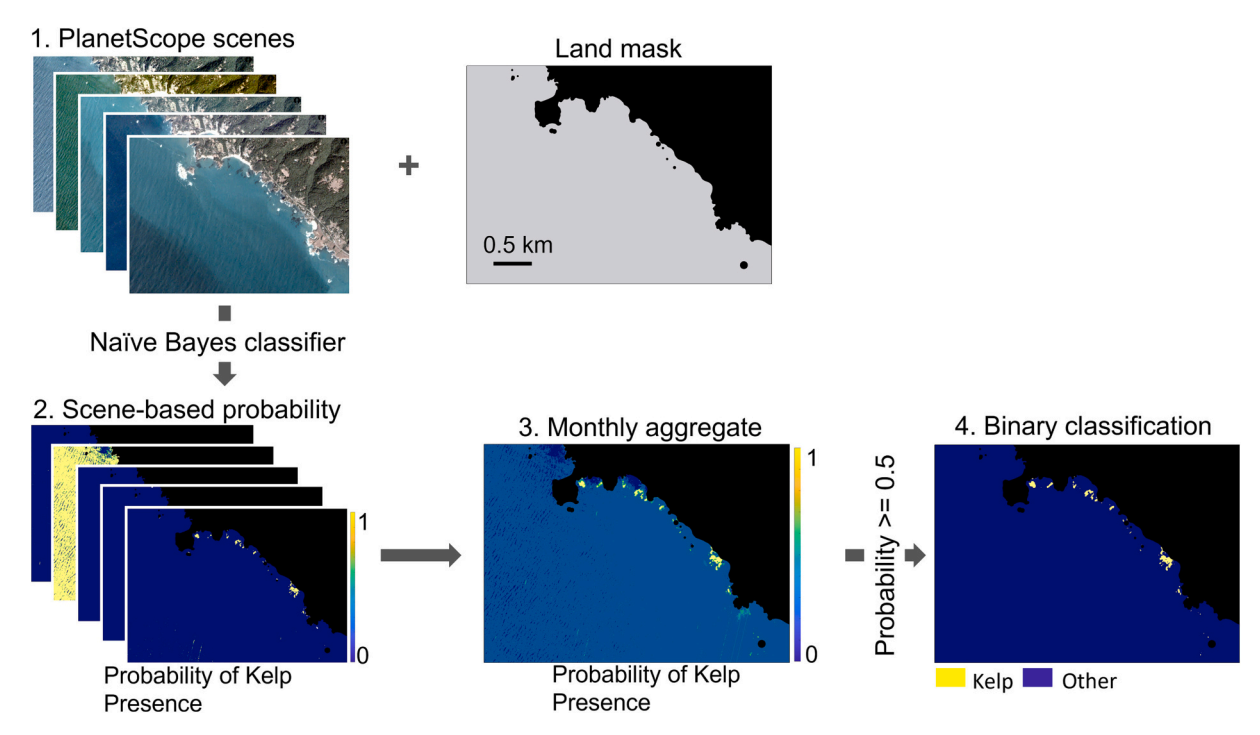


Fig. 3. Conceptual diagram of the automated portion of the kelp canopy detection scheme. Binary classifications were manually edited to remove any potential remaining image artifacts.

validation dataset included high resolution kelp canopy classifications derived from occupied aircraft surveys hosted through CDFW. CDFW aerial surveys were collected between late summer and winter. The first aerial survey was conducted in 1989, and the second was conducted in 1999. They began collecting aerial data annually from 2002 to 2016, although some years and regions were not completed due to budget constraints, cloud cover, inclement weather, etc. (CDFW, 2021). The surveys contain complete coverage of Sonoma and Mendocino counties for 9 years (1989, 1999, 2003-2005, 2008, and 2014-2016), with partial coverage for 4 years (2002, 2009, 2010, and 2013). The data were originally collected at ~25 cm and were later resampled to 2 m internally at CDFW. PlanetScope data and CDFW data spatially overlap in 2016, and these data were used for comparison of kelp canopy area estimates. We converted the 2016 CDFW classification from a shapefile to 3 m pixels corresponding to the 3 m grid of PlanetScope imagery. We binned the northern California coastline into 1 km coastline segments and calculated the total kelp canopy area in each segment estimated by both CDFW and PlanetScope. CDFW data distinguish floating and submerged kelp canopy, and the submerged canopy class was excluded from the validation analysis.

The second validation dataset included classifications derived from UAV surveys of kelp canopy that were conducted along the coastline of Mendocino and Sonoma counties in 2019 (number of samples (n) = 25), 2020 (n=32), and 2021 (n=34; Saccomanno et al., 2022). The surveyed sites varied in size from 0.16 to 1.48 km². Expert classifiers manually selected and applied thresholds to the Red-Blue vegetation index used to derive kelp canopy in all UAV images, with a final resolution of ~ 3 cm (Cavanaugh et al., 2021a). We extracted the overlapping areas between each UAV surveyed site and the respective PlanetScope classifications and performed a site level comparison of kelp canopy area.

Last, we performed validations against Landsat satellite imagery

(Bell et al., 2022). In this dataset, bull kelp canopy was estimated at 30 m resolution from 1984 to 2021 at quarterly intervals following methods from Cavanaugh et al., 2011 and Bell et al., 2020. Briefly, a binary decision tree was applied to Landsat Level 2 Surface Reflectance images to identify canopy presence, and MESMA was applied to pixels with canopy presence to estimate fractional coverage of kelp and seawater (Bell et al., 2020). We extracted and composited Landsat-derived classifications from the third (July to September) and fourth (October to December) quarter of each year between 2016 and 2021. We binned the northern California coastline into 1 km coastline segments and calculated the total kelp canopy area in each segment estimated by both Landsat and PlanetScope. The CDFW, UAV, and PlanetScope datasets each represented kelp coverage as presence/absence, and to maintain consistency, the Landsat dataset was converted to presence/absence. If a Landsat pixel contained kelp canopy area above 0, kelp was considered present in that pixel (900 m^2) .

2.6. Effect of spatial scale on refugia detection

Each dataset has its own lower detection limit of kelp canopy, and quantifying subpixel detection limits has implications for the local and regional application of aerial estimates. Calculating these uncertainties is often performed using comparisons against higher resolution sensors, which likely provide estimates closer to 'ground truth' data (Wang and Hu, 2021). To determine the effect of spatial scale on refugia detection, we used the UAV-based classifications to calculate the percentage of a PlanetScope pixel (9 m²) and a Landsat pixel (900 m²) that needs to be occupied by kelp canopy for the classification scheme to detect kelp presence. These calculations could not be performed for CDFW data, as they did not temporally overlap with any of the UAV flights. We identified all pixels that were misidentified as 'not kelp' in the PlanetScope and Landsat classifications (false negatives) when compared to overlapping UAV pixels that estimated canopy presence in the same location. Of this subset, we randomly selected pixels that were 150 m apart to minimize the effects of spatial autocorrelation in the pixel-wise analyses. We calculated the percentage of the PlanetScope and Landsat pixels that were occupied by kelp canopy in the UAV images and used the pixel fractions to determine a threshold for refugia detection.

2.7. Distribution of refugia

Bull kelp on the north coast of California has been characterized by a prolonged collapse, and a multi-year perspective can provide insight to where, and why, remnant populations have been able to persist. We define refugia as persistent kelp pixels that occurred in at least three of the six years immediately following the marine heatwave between 2016 and 2021. For 2016, we used kelp locations in both the CDFW and PlanetScope classifications. The three occurrences did not have to be consecutive.

To find the maximum historical kelp canopy extent observed prior to the marine heatwave, we merged the extents of all CDFW aerial survey shapefiles that identified floating canopy (with either total or partial coverage of the study area) taken between 1989 and 2015. The maximum historical kelp canopy extent was used as a proxy for kelp habitat, i.e., any place that kelp canopy has been observed in the historical record. The maximum extent shapefile was converted to a raster with a pixel size of 3 m corresponding to the 3 m grid of PlanetScope imagery. We used these data to identify pixels that have been occupied by kelp canopy in the past, representing suitable kelp habitat but not refugia.

3. Results

3.1. Kelp canopy classification and validation

The training data for the Naïve Bayes classifier consisted of 93

images, which included data from 57 different satellites across 3 satellite cohorts (0e, 0f, 10). The log residual correction helped to increase separability between kelp and water classes in the training data across each satellite cohort, particularly in the blue and green bands compared to raw reflectance values (Fig. 4). The log residual correction also lowered the average coefficient of variation for the wavelengths in both the kelp (43.82 and 14.86, respectively) and water (45.90 and 8.06, respectively) classes. The kelp class exhibited high variability in the NIR before and after the correction was applied, but the values were higher than water on average (Fig. 4). The correction was applied to 2070 images, which included data from 187 satellites across 4 satellite families (0e, 0f, 10, 20).

The PlanetScope-derived kelp canopy estimates agreed with regional CDFW classifications ($R^2=0.38,\,p<0.001,\,{\rm slope}=0.61;\,{\rm Fig.~5b})$ and regional Landsat classifications ($R^2=0.49,\,p<0.001,\,{\rm slope}=1.00;\,{\rm Fig.~5c})$ based on 1 km coastline partitions. PlanetScope estimates were also strongly correlated with UAV estimates of kelp area at the site level ($R^2=0.70,\,p<0.001,\,{\rm slope}=0.84;\,{\rm Fig.~5a})$. PlanetScope underestimated kelp canopy area compared to UAV in 2019 and 2020, but overestimated canopy area in 2021. False positives were rarely identified in the PlanetScope data compared to UAV (2% of all water pixels across all years).

All three comparisons had the best agreement when kelp canopy area was relatively high (between 0.1 and 1 km²). However, differences in estimates were most pronounced in locations with low kelp canopy. To characterize these differences, we found the pixels that were misidentified as water in the PlanetScope and Landsat classifications when compared to overlapping UAV pixels that estimated canopy presence. We plotted the number of false negative detections as a function of percent occupancy within that pixel (identified from the UAV classifications) and found that the number of false negatives exponentially decayed as the percent occupancy of kelp within a PlanetScope and Landsat pixel increased (Fig. 6). For both PlanetScope and Landsat, the number of false negative detections began to converge to 0 when kelp occupancy was close to 20% of a single pixel (1.8 m² for PlanetScope and 180 m² for Landsat; Fig. 6). This agrees with previous work that demonstrated Landsat has a higher likelihood of missing a pixel that contains kelp if it is occupied by <20% kelp canopy (Hamilton et al., 2020). Landsat missed nearly twice as many kelp pixels than Planet-Scope at very low percent occupancy (i.e., <10%; Fig. 6).

3.2. Kelp canopy time series

The combined effects of a marine heatwave and overgrazing of urchins led to a collapse in bull kelp abundance along the north coast of California (Rogers-Bennett and Catton, 2019), and there was a pronounced lack of bull kelp recovery through 2021, with kelp abundance remaining at historically low levels (Fig. 7). Generally, there was good correspondence among Landsat, CDFW, and PlanetScope estimates, indicating that each method is adequate for analyzing kelp abundance at regional scale. Landsat and CDFW data both agreed that bull kelp canopy showed high interannual variability in the years leading up to the heatwave (1984 to 2013), although Landsat provided a much more comprehensive record of canopy abundance during this period (n = 30) compared to CDFW (n = 6). After the onset of the heatwave in 2014, Landsat and CDFW both detected large losses, which were sustained throughout the duration of the heatwave. CDFW and PlanetScope only overlap in 2016, but the two have generally good agreement (1.21 and 1.18 km², respectively). In late 2016 and early 2017, temperature anomalies began returning to near-normal levels (McPherson et al., 2021). However, kelp populations only slightly recovered from 2017 to 2021. PlanetScope was able to consistently detect a higher annual abundance than Landsat (0.9 km² on average) despite the low abundance present.

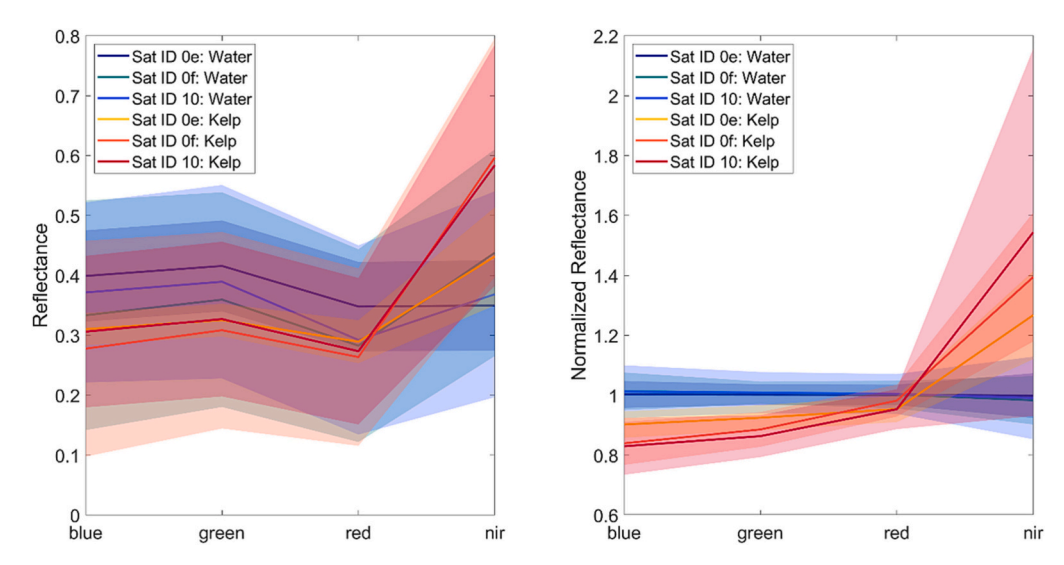


Fig. 4. Mean reflectance (solid line) and standard deviation (shaded region) of training data for each satellite cohort (0e, 0f, and 10) before (left) and after (right) the log residual correction was applied.

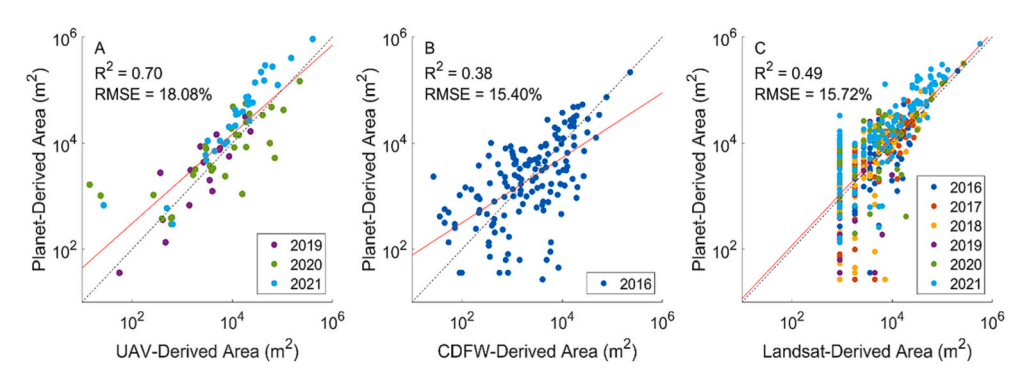


Fig. 5. Comparison of bull kelp canopy area estimates between PlanetScope and data from UAV (A), CDFW (B), and Landsat (C) between overlapping locations. Dataset pairs were captured using different temporal aggregations (UAV and CDFW = daily, PlanetScope = monthly, Landsat = quarterly), but each cover at least one day during the peak kelp canopy season in northern California (September to October). The dotted line shows 1:1 relationship, while the red lines are the linear fits in log space. (For interpretation of the references to color in this figure legend, the reader is referred to the web version of this article.)

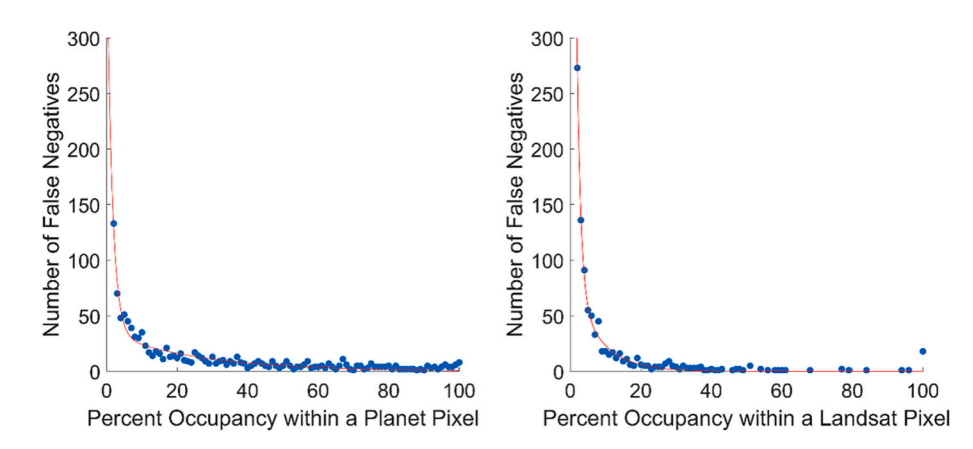


Fig. 6. Number of false negative kelp detections from both PlanetScope (left) and Landsat (right) as a function of the percent occupancy identified from the UAV classifications.

3.3. Distribution of refugia

In Sonoma and Mendocino counties, there was a total of $35.97 \, \mathrm{km}^2$ of suitable bull kelp habitat, as defined by areas where kelp canopy was present during at least one year between 1989 and 2021. We identified $0.718 \, \mathrm{km}^2$ of kelp refugia (areas where kelp was present in at least 3 of the 6 years between 2016 and 2021), comprising 2% of the total available habitat and 9.4% of the average canopy area observed prior to 2014

from CDFW. To assess spatial patterns in refugia occupancy across the study area, we aggregated the data to 1 km \times 1 km grid cells and calculated the abundance of refugia compared to the abundance of historical habitat within each grid cell (Fig. 8). Refugia were almost completely absent in the northern portion of the study area between a latitudinal range of 39°3′ to 40°0′, aside from a few small, persistent beds near Point Delgada and Abalone Point (Fig. 8). Refugia abundance increased just north of Noyo Bay to Elk, where 61.6% of the 1 km grid

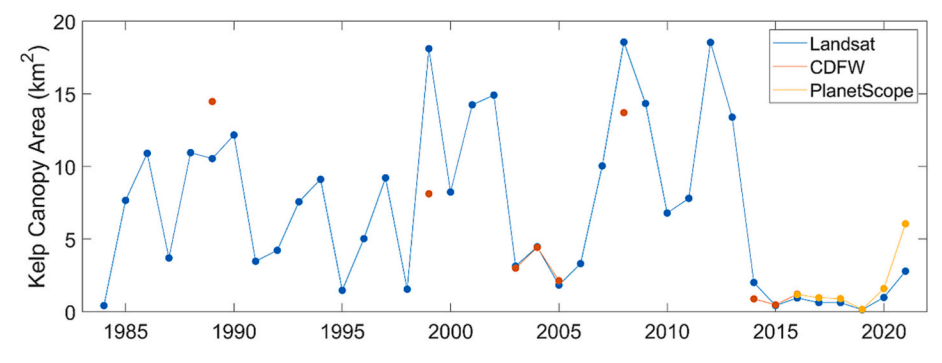


Fig. 7. Kelp canopy area in northern California from 1984 to 2021 from Landsat, CDFW, and Planet-Scope derived estimates. CDFW and PlanetScope overlap in 2016, but the two have generally good agreement (1.21 and 1.18 km², respectively).

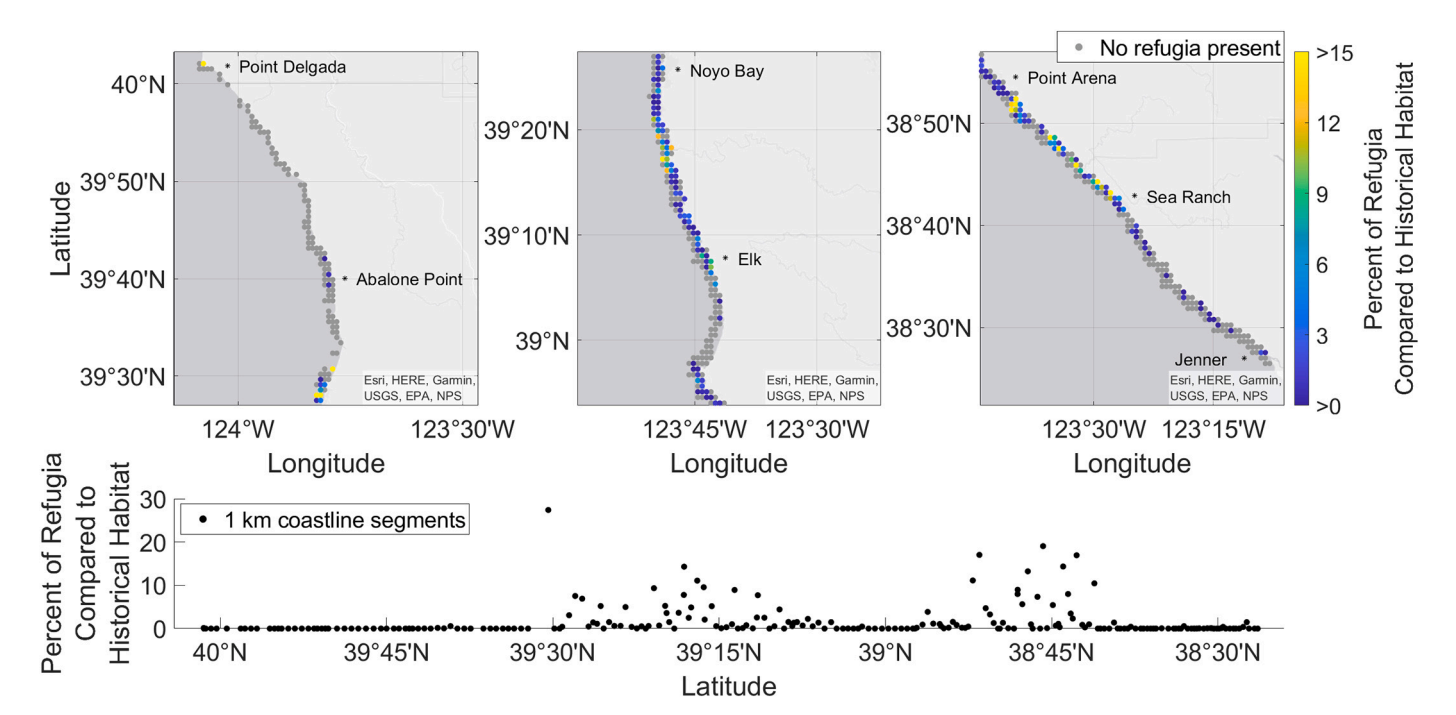


Fig. 8. The percentage of bull kelp refugia occupancy in 1 km grid cells compared to available habitat in the same locations from the northernmost (left) to southernmost (right) portions of the study area. Gray areas represent locations that were historically occupied by kelp canopy but were not occupied by refugia. The bottom panel represents the latitudinal variation in refugia occupancy from north to south along 1 km coastline segments.

cells were occupied by refugia at abundances ranging from 0.01 to 36.23% of total available habitat. However, refugia occupied $<\!3\%$ of potential habitat in this area on average (2.52% \pm 5.19%). Refugia were sparsely populated south of Elk through Point Arena, where occupancy increased again along the coastline to Sea Ranch (Fig. 8). From Point Arena to Sea Ranch, 54.55% of the 1 km grid cells were occupied by refugia at abundances ranging from 0.05 to 34.36% of total available habitat. Here, refugia occupied a slightly higher percentage of potential habitat than the region between Noyo Bay and Elk on average (6.66% \pm 7.67%). Refugia presence decreased in the southern portion of the study area from Sea Ranch to Jenner, where only 19.39% of grid cells were occupied, with a maximum occupancy of just 2.14% (Fig. 8).

4. Discussion

4.1. Comparison of kelp canopy detection approaches

Our new method for mapping bull kelp canopy from Planet satellite imagery demonstrates that CubeSat data are an effective tool for detection and regional monitoring during years of low kelp canopy coverage and density. The PlanetScope-derived kelp canopy estimates were similar to maps created from high resolution occupied and unoccupied aerial surveys, as well as the Landsat satellites. We expected variation in kelp canopy estimates among each dataset, as the method of detection and spatial and temporal resolutions differed, and therefore so did their detection capability of floating canopy. The method we present in this manuscript relied on developing relationships between kelp canopy area and image-derived spectral features (i.e., band reflectance values) using manually classified data for training points. We found it difficult to create robust classifiers or models that were accurate across different images and satellites, but our spectral normalization and temporal aggregation scheme helped address the radiometric and geometric inconsistencies both within and between PlanetScope satellite images. Our monthly composite classifications provide spatially and temporally continuous maps of bull kelp coverage at finer scale than previously possible. These approaches could be applied to other applications where increased noise or geolocation inaccuracy in individual images caused a propagation of errors during classification (Cannistra et al., 2021; Wicaksono and Lazuardi, 2018; Xu et al., 2020).

PlanetScope consistently underestimated kelp canopy area compared

to UAV classifications in 2019 and 2020, which can be explained by the resolution mismatch between the two datasets. Kelp canopy was the lowest on record in northern California in 2019 and remained low in 2020, resulting in few areas with high kelp abundance. The stipes and blades of the sparsely populated bull kelp individuals were visible in the UAV imagery, and therefore these data were able to capture nearly all floating kelp canopy present at each site. For PlanetScope, the classifications were most comparable to UAV when kelp occupancy was greater than or equal to 20% of a single pixel (i.e., $\sim 1.8 \text{ m}^2$ of kelp), and so kelp coverage was likely lower than this threshold in many areas during 2019 and 2020. However, there were some signs of recovery in 2021, with increased bull kelp coverage and densities along the coastline. Planet-Scope consistently overestimated kelp canopy compared to UAV during this period. The PlanetScope classifications provide a presence/absence metric and do not describe the amount of canopy coverage at the pixel level. Here, there was likely a higher proportion of pixels occupied by <100% canopy coverage, resulting in overclassifications compared to UAV.

Although the CDFW and PlanetScope classifications offered similar spatial resolutions (2 m and 3 m, respectively) there were greater differences between PlanetScope and CDFW along sections of coastline with low bull kelp abundance. The CDFW classifications were derived from aerial data collected on a single date, while the PlanetScope classifications were generated from multiple images throughout September and October of each year. As a result, these datasets were not representing canopy conditions under equivalent tidal height and current stages, which have the potential to impact the amount of kelp detected on the surface. As tidal height and current speeds increase, they can significantly reduce the amount of kelp canopy present (Britton-Simmons et al., 2008; Cavanaugh et al., 2021a), which may have contributed to the variability at lower kelp abundances. Additionally, there are several scenarios that could occur for the PlanetScope-based classifications to exclude kelp from a region with kelp presence. For example, if a large kelp bed were present and detected by PlanetScope in one image in the beginning of the month, but a wave event caused mass dislodgement and mortality, the remainder and majority of the month would have no kelp canopy presence, resulting in a monthly classification of no kelp canopy presence (despite the classification scheme containing one accurate detection).

The 35+ year archive of Landsat data provides a spatially and temporally consistent record of kelp canopy coverage (Wulder et al., 2012). Cost-free access to the Landsat archive since 2008 has allowed for significant methodological and ecological advancements in kelp remote sensing (Kennedy et al., 2014), including the creation of seamless data products in formats suitable for non-experts (i.e., Bell et al., 2022). While commercial optical sensors such as PlanetScope have provided new opportunities for mapping kelp canopy at finer spatial scale than the Landsat archive (Pettorelli et al., 2014), the costs associated with the data may not be feasible for some research projects that require long-term monitoring of ecological processes, which occur over decades to centuries and at spatial scales across hundreds of kilometers (Reed et al., 2016). The choice of remote sensing and analytic data approaches are dependent upon research objectives and duration of funding (Cavanaugh et al., 2021b).

For example, Landsat has been shown to significantly underestimate the amount of floating bull kelp canopy during years of low abundance, including during the 2014 to 2016 marine heatwave (Finger et al., 2021). At a local scale, Landsat was unable to capture refugia if they occupied <20% of a pixel (180 m²). This limitation reduces the potential of Landsat for capturing the spatial complexity of refugia (i.e., small, sparse, and fringing beds) or even identifying their presence altogether. Refugia dynamics require a sensor that can capture fine scale patterns in kelp bed size, shape, and area - particularly in populations that are relatively close to the coastline, which is a challenge for moderate resolution sensors (Bell et al., 2020; Finger et al., 2021; Hamilton et al., 2020). Despite methodological differences, the general agreement

between PlanetScope, UAV, CDFW, and Landsat-based classifications supports its applicability for detecting refugia.

The spatial and temporal coverage of PlanetScope data make them a favorable monitoring resource in the coastal zone, as regional imagery is available for download in near real time. Coastal variability is influenced by drivers that operate on timescales of hours (i.e., tides) to days (i.e., marine heatwaves and storm events) to decades (i.e., sea level rise and ocean acidification), and the magnitude of change can range from centimeters to hundreds of kilometers (Muller-Karger et al., 2018). Due to the dynamic nature and spatial complexity of coastal targets, this study has demonstrated that the high-frequency sampling and high spatial resolution provided by PlanetScope CubeSats has been a successful resource for mapping bull kelp. Other studies have demonstrated the applicability of CubeSat constellation data for other coastal foundation species, including seagrasses (Tamondong et al., 2018; Wicaksono and Lazuardi, 2018) and corals (Asner et al., 2017; Li et al., 2020; Yamano et al., 2020). In contrast, the CDFW surveys were not completed during some years and regions due to budget constraints, cloud cover, inclement weather, etc., and the last successful survey was completed in 2016 (CDFW, 2021). The spatial and temporal coverage of drone operations are limited by battery life, wind, weather, and regulatory limitations (Gray et al., 2022) making them inefficient for monitoring efforts over large scales. While the Landsat satellites provide the most spatially and temporally comprehensive dataset, they have a higher detection limit than PlanetScope, introducing complications for refugia detection.

4.2. Distribution of bull kelp refugia

In 2014, the once extensive and persistent bull kelp forests in northern California shifted to urchin barrens (Rogers-Bennett and Catton, 2019). Our analysis of PlanetScope imagery showed that there was a pronounced lack of bull kelp recovery through 2020, with some potential recovery in 2021, although kelp abundance still remained at historically low levels. However, we identified pockets of refugia that persisted throughout the marine heatwave and urchin outbreak. There is evidence that refugia function as source populations for extirpated locations that were more sensitive to disturbance within kelp and other ecological communities, which is the first step for species recolonization (Johnson and Mann, 1988; Landesmann and Morales, 2018). However, environmental conditions impact both the persistence of refugia and the subsequent success of re-establishment, making refugia locations and their environmental drivers valuable information for monitoring, conservation, and restoration efforts (Wilson et al., 2020).

Between 2016 and 2021, northern California bull kelp refugia occupied 0.718 km² of the coastline. This accounted for about 2% of the total available kelp habitat in the region, and about 9.4% of the average canopy area observed prior to 2014. In a recent publication, McPherson et al. (2021) documented the spatial and temporal variability of bull kelp canopy area in northern California from 1985 to 2019 along 90 m latitudinal bins, and their patterns of kelp abundance were closely related to our maps of refugia presence north of Point Arena. For example, a small abundance of bull kelp refugia was found from Fort Delgada to Noyo Bay and from Elk to Point Arena. McPherson et al. (2021) show a lack of persistence of kelp canopy along the same latitudinal gradients, which indicates that these areas were unsuitable for bull kelp growth during most years in their time series and were not disproportionately impacted by the effects of the heatwave. However, a small abundance of bull kelp refugia was also found south of Point Arena from Sea Ranch to Jenner. While McPherson et al. (2021) show low kelp canopy abundances in this region after 2014, the area displays high persistence throughout the rest of the time series (1985 to 2013), indicating that the area was suitable for persistent historical kelp growth, but was unsuitable for refugia.

5. Conclusion

In 2014, the once extensive and persistent bull kelp forests in northern California shifted to urchin barrens. This study demonstrates strong potential for using CubeSat data for monitoring these regional bull kelp populations with local-level precision. Using these data, we show that northern California has continued to support refuge bull kelp populations despite widespread and unprecedented declines. As a foundation species, understanding the local-scale factors that support bull kelp refugia are important for informed protection and management, helping to ensure the future of this species as it continues to face climate variability and change.

Credit author statement

Ka.C.C. and Ky.C.C. conceptualized the study. Ka.C.C., C.C.P., and V. R.S. organized and processed the remote sensing imagery, and Ka.C.C. and T.W.B. performed validation of the methods. Ka.C.C. conducted the analysis and Ky.C.C. helped to assess and interpret the results. Ka.C.C. prepared the original draft and all authors reviewed and edited the manuscript.

Declaration of Competing Interest

The authors declare that they have no known competing financial interests or personal relationships that could have appeared to influence the work reported in this paper.

Data availability

Data will be made available on request.

Acknowledgements

This work was supported by The Nature Conservancy, Ocean Protection Council, and NASA Ocean Biology & Biogeochemistry [80NSSC21K1429]. The authors would like to acknowledge the Planet Open California program and the Planet Education and Research program, which provided data for the early stages of this research. We would like to thank the field and laboratory technicians who helped in the collection and processing of the PlanetScope and UAV data.

References

- Abbott, I.A., Hollenberg, G.J., 1992. Marine Algae of California. Stanford University Press.
- Ahmad, A., Quegan, S., 2012. Analysis of maximum likelihood classification on multispectral data. Appl. Math. Sci. 6, 6425–6436.
- Ahmad, A., Sakidin, H., Sari, M.Y.A., Amin, A.R.M., Sufahani, S.F., Rasib, A.W., 2021. Naïve Bayes classification of high-resolution aerial imagery. Int. J. Adv. Comput. Sci. Appl. 12, 168–177.
- Andrew, M.E., Warrener, H., 2017. Detecting microrefugia in semi-arid landscapes from remotely sensed vegetation dynamics. Remote Sens. Environ. 200, 114–124.
- Ashcroft, M.B., 2010. Identifying refugia from climate change. J. Biogeogr. 37, 1407–1413.
- Asner, G.P., Martin, R.E., Mascaro, J., 2017. Coral reef atoll assessment in the South China Sea using Planet Dove satellites. Remote. Sens. Ecol. Conserv. 3, 57–65.
- Asner, G.P., Vaughn, N.R., Martin, R.E., Foo, S.A., Heckler, J., Neilson, B.J., Gove, J.M., 2022. Mapped coral mortality and refugia in an archipelago-scale marine heat wave. Proc. Natl. Acad. Sci. U. S. A. 119, e2123331119.
- Bell, T.W., Allen, J.G., Cavanaugh, K.C., Siegel, D.A., 2020. Three decades of variability in California's giant kelp forests from the Landsat satellites. Remote Sens. Environ. 238, 110811.
- Bell, T.W., Cavanaugh, K.C., Siegel, D.A., 2022. SBC LTER: Time series of quarterly NetCDF files of kelp biomass in the canopy from Landsat 5, 7 and 8, since 1984 (ongoing) ver. 18. Environmental Data Initiative. https://doi.org/10.6073/pasta/5fa36b985f30ee04d4771af2288aedd4.
- Blowes, S.A., Supp, S.R., Antão, L.H., Bates, A., Bruelheide, H., Chase, J.M., Moyes, F., Magurran, A., McGill, B., Myers-Smith, I.H., Winter, M., Bjorkman, A.D., Bowler, D. E., Byrnes, J.E.K., Gonzalez, A., Hines, J., Isbell, F., Jones, H.P., Navarro, L.M., Thompson, P.L., Vellend, M., Waldock, C., Dornelas, M., 2019. The geography of biodiversity change in marine and terrestrial assemblages. Science 366, 339–345.

- Bond, N.A., Cronin, M.F., Freeland, H., Mantua, N., 2015. Causes and impacts of the 2014 warm anomaly in the NE Pacific. Geophys. Res. Lett. 42, 3414–3420.
- Britton-Simmons, K., Eckman, J.E., Duggins, D.O., 2008. Effect of tidal currents and tidal stage on estimates of bed size in the kelp Nereocystis luetkeana. Mar. Ecol. Prog. Ser. 335, 95–105.
- Cacciapaglia, C., van Woesik, R., 2015. Reef-coral refugia in a rapidly changing ocean. Glob. Change Biol. 21, 2272–2282.
- Cavanaugh, K.C., Bell, T., Costa, M., Eddy, N.E., Gendall, L., Gleason, M.G., Hessing-Lewis, M., Martone, R., McPherson, M., Pontier, O., Reshitnyk, L., Beas-Luna, R., Carr, M., Caselle, J.E., Cavanaugh, K.C., Flores Miller, R., Hamilton, S., Heady, W.N., Hirsh, H.K., Hohman, R., Lee, L.C., Lorda, J., Ray, J., Reed, D.C., Saccomanno, V.R., Schroeder, S.B., 2021b. A review of the opportunities and challenges for using remote sensing for management of surface-canopy forming kelps. Front. Mar. Sci. 8, 753531.
- Cavanaugh, K.C., Cavanaugh, K.C., Bell, T.W., Hockridge, E.G., 2021a. An automated method for mapping giant kelp canopy dynamics from UAV. Front. Environ. Sci. 8, 587354.
- Cavanaugh, K.C., Siegel, D.A., Reed, D.C., Dennison, P.E., 2011. Environmental controls of giant-kelp biomass in the Santa Barbara Channel, California. Mar. Ecol. Prog. Ser. 429 1–17
- California Department of Fish and Wildlife, 2021. Aerial Kelp Surveys. https://wildlife.ca.gov/Conservation/Marine/Kelp/Aerial-Kelp-Surveys.
- Cannistra, A.F., Shean, D.E., Cristea, N.C., 2021. High-resolution CubeSat imagery and machine learning for detailed snow-covered area. Remote Sens. Environ. 258, 112399
- Chen, I.-C., Hill, J.K., Ohlemüller, R., Roy, D.B., Thomas, C.D., 2011. Rapid range shifts of species associated with high levels of climate warming. Science 333, 1024–1026.
- Dixon, D.J., Callow, J.N., Duncan, J.M.A., Setterfield, S.A., Pauli, N., 2021. Satellite prediction of forest flowering phenology. Remote Sens. Environ. 255, 112197.
- Dobrowski, S.Z., 2011. A climatic basis for microrefugia: the influence of terrain on climate. Glob. Change Biol. 17, 1022–1035.
- Elsmore, K., Nickols, K.J., Ford, T., Cavanaugh, K.C., Cavanaugh, K.C., Gaylord, B., 2022.
 Macrocystis pyrifera forest development shapes the physical environment through current velocity reduction. Mar. Ecol. Prog. Ser. 694, 45–59.
- Finger, D.J.I., McPherson, M.L., Houskeeper, H.F., Kudela, R.M., 2021. Mapping bull kelp canopy in northern California using Landsat to enable long-term monitoring. Remote Sens. Environ. 254, 112243.
- Frazier, A.E., Hemingway, B.L., 2021. A technical review of planet smallsat data: practical considerations for processing and using PlanetScope imagery. Remote Sens. 13, 3930.
- Ganesh, B.P., Aravindan, S., Raja, S., Thirunavukkarasu, A., 2013. Hyperspectral satellite data (Hyperion) preprocessing—a case study on banded magnetite quartzite in Godumalai Hill, Salem, Tamil Nadu, India. Arab. J. Geosci. 6, 3249–3256.
- Gray, P.C., Larsen, G.D., Johnston, D.W., 2022. Drones address an observational blind spot for biological oceanography. Front. Ecol. Environ. https://doi.org/10.1002/ fee.2472.
- Green, A.A., Craig, M.D., 1985. Analysis of aircraft spectrometer data with logarithmic residuals. In: JPL Proc. of the Airborne Imaging Spectrometer Data Anal. Workshop.
- Hamilton, S.L., Bell, T.W., Watson, J.R., Grorud-Colvert, K.A., Menge, B.A., 2020.Remote sensing: generation of long-term kelp bed data sets for evaluation of impacts of climatic variation. Ecology 101, e03031.
- Harvell, C.D., Montecino-Latorre, D., Caldwell, J.M., Burt, J.M., Bosley, K., Keller, A., Heron, S.F., Salomon, A.K., Lee, L., Pontier, O., Pattengill-Semmens, C., Gaydos, J.K., 2019. Disease epidemic and a marine heat wave are associated with the continental-scale collapse of a pivotal predator (Pycnopodia helianthoides). Sci. Adv. 5, eaai/7042
- Johnson, C.R., Mann, K.H., 1988. Diversity, patterns of adaptation, and stability of Nova Scotian kelp beds. Ecol. Monogr. 58, 129–154.
- Kavousi, J., Keppel, G., 2018. Clarifying the concept of climate change refugia for coral reefs. ICES J. Mar. Sci. 75, 43–49.
- Kennedy, R.E., Andréfouët, S., Cohen, W.B., Gómez, C., Griffiths, P., Hais, M., Healey, S. P., Helmer, E.H., Hostert, P., Lyons, M.B., Meigs, G.W., Pflugmacher, D., Phinn, S.R., Powell, S.L., Scarth, P., Sen, S., Schroeder, T.A., Schneider, A., Sonnenschein, R., Vogelmann, J.E., Wulder, M.A., Zhu, Z., 2014. Bringing an ecological view of change to Landsat-based remote sensing. Front. Ecol. Environ. 12, 339–346.
- Keppel, G., Van Niel, K.P., Wardell-Johnson, G.W., Yates, C.J., Byrne, M., Mucina, L., Schut, A.G.T., Hopper, S.D., Franklin, S.E., 2012. Refugia: identifying and understanding safe havens for biodiversity under climate change. Glob. Ecol. Biogeogr. 21, 393–404.
- Kranjčić, N., Medak, D., 2020. Evaluating different machine learning methods on RapidEye and PlanetScope satellite imagery. Geodetski List 74, 1–18.
- Landesmann, J.B., Morales, J.M., 2018. The importance of fire refugia in the recolonization of a fire-sensitive conifer in northern Patagonia. Plant Ecol. 219, 455–466
- Latte, N., Lejeune, P., 2020. PlanetScope radiometric normalization and Sentinel-2 superresolution (2.5 m): a straightforward spectral-spatial fusion of multi-satellite multisensor images using residual convolutional neural networks. Remote Sens. 12, 2366.
- Leach, N., Coops, N.C., Obrknezev, N., 2019. Normalization method for multi-sensor high spatial and temporal resolution satellite imagery with radiometric inconsistencies. Comput. Electron. Agric. 164, 104893.
- Li, J., Knapp, D.E., Fabina, N.S., Kennedy, E.V., Larsen, K., Lyons, M.B., Murray, N.J., Phinn, S.R., Roelfsema, C.M., Asner, G.P., 2020. A global coral reef probability map generated using convolutional neural networks. Coral Reefs 39, 1805–1815.
- McPherson, M.L., Finger, D.J.I., Houskeeper, H.F., Bell, T.W., Carr, M.H., Rogers-Bennett, L., Kudela, R.M., 2021. Large-scale shift in the structure of a kelp forest ecosystem co-occurs with an epizootic and marine heatwave. Commun. Biol. 4, 298.

- Miller, K.A., Estes, J.A., 1989. Western range extension for Nereocystis luetkeana in the North Pacific Ocean. Bot. Mar. 32, 535–538.
- Muller-Karger, F.E., Hestir, E., Ade, C., Turpie, K., Roberts, D.A., Siegel, D., Miller, R.J., Humm, D., Izenberg, N., Keller, M., Morgan, F., Frouin, R., Dekker, A.G., Gardner, R., Goodman, J., Schaeffer, B., Franz, B.A., Pahlevan, N., Mannino, A.G., Concha, J.A., Ackleson, S.G., Cavanaugh, K.C., Romanou, A., Tzortziou, M., Boss, E.S., Pavlick, R., Freeman, A., Rousseaux, C.S., Dunne, J., Long, M.C., Klein, E., McKinley, G.A., Goes, J., Letelier, R., Kavanaugh, M., Roffer, M., Bracher, A., Arrigo, K.R., Dierssen, H., Zhang, X., Davis, F.W., Best, B., Guralnick, R., Moisan, J., Sosik, H.M., Kudela, R., Mouw, C.B., Barnard, A.H., Palacios, S., Roesler, C., Drakou, E.G., Appeltans, W., Jetz, W., 2018. Satellite sensor requirements for monitoring essential biodiversity variables of coastal ecosystems. Ecol. Appl. 28, 749–760.
- Nicholson, N.L., 1970. Field studies on the giant kelp Nereocystis 1, 2. J. Phycol. 6, 177–182.
- Oliver, E.C.J., Donat, M.G., Burrows, M.T., Moore, P.J., Smale, D.A., Alexander, L.V., Benthuysen, J.A., Feng, M., Sen Gupta, A., Hobday, A.J., Holbrook, N.J., Perkins-Kirkpatrick, S.E., Scannell, H.A., Straub, S.C., Wernberg, T., 2018. Longer and more frequent marine heatwaves over the past century. Nat. Commun. 9, 1324.
- Park, D.C., 2016. Image classification using naïve bayes classifier. Int. J. Comput. Sci. Electron. Eng. 4, 135–139.
- Pettorelli, N., Laurance, W.F., O'Brien, T.G., Wegmann, M., Nagendra, H., Turner, W., 2014. Satellite remote sensing for applied ecologists: opportunities and challenges. J. Appl. Ecol. 51, 839–848.
- Planet, 2021. Planet Imagery Product Specifications.
- Reed, D.C., Rassweiler, A.R., Miller, R.J., Page, H.M., Holbrook, S.J., 2016. The value of a broad temporal and spatial perspective in understanding dynamics of kelp forest ecosystems. Mar. Freshw. Res. 67, 14–24.
- Rogers-Bennett, L., Catton, C.A., 2019. Marine heat wave and multiple stressors tip bull kelp forest to sea urchin barrens. Sci. Rep. 9, 15050.
- Rosenzweig, C., Karoly, D., Vicarelli, M., Neofotis, P., Wu, Q., Casassa, G., Menzel, A., Root, T.L., Estrella, N., Seguin, B., Tryjanowski, P., Liu, C., Rawlins, S., Imeson, A., 2008. Attributing physical and biological impacts to anthropogenic climate change. Nature 453, 353–357.
- Roy, D.P., Huang, H., Houborg, R., Martins, V.S., 2021. A global analysis of the temporal availability of PlanetScope high spatial resolution multi-spectral imagery. Remote Sens. Environ. 264, 112586.
- Saccomanno, V.R., Bell, T., Pawlak, C., Stanley, C.K., Cavanaugh, K.C., Hohman, R., Klausmeyer, K.R., Cavanaugh, K., Nickels, A., Hewerdine, W., Garza, C., Fleener, G., Gleason, M., 2022. Using unoccupied aerial vehicles to map and monitor changes in

- emergent kelp canopy after an ecological regime shift. Remote Sens. Ecol. Conserv. 0, 62, 75
- Schroeder, S.B., Boyer, L., Juanes, F., Costa, M., 2019. Spatial and temporal persistence of nearshore kelp beds on the west coast of British Columbia, Canada using satellite remote sensing. Remote Sens. Ecol. Conserv. 6, 327–343.
- Tamondong, A.M., Cruz, C.A., Guihawan, J., Garcia, M., Quides, R.R., Cruz, J.A., Blanco, A.C., 2018. Remote sensing-based estimation of seagrass percent cover and LAI for above ground carbon sequestration mapping. Proc. SPIE 10778, 1077803-1.
- Timmer, B., Reshitnyk, L.Y., Hessing-Lewis, M., Juanes, F., Costa, M., 2022. Comparing the use of red-edge and near-infrared wavelength ranges for detecting submerged kelp canopy. Remote Sens. 14, 2241.
- Traganos, D., Cerra, D., Reinartz, P., 2017. Cubesat-derived Detection of Seagrasses using Planet Imagery following unmixing-based Denoising: Is small the next big? ISPRS Archives. XLII-1/W1 283–287.
- Vadas, R.L., 1972. Ecological implications of culture studies on Nereocystis Luetkeana 1. J. Phycol. 8, 196–203.
- Veisze, P., Kilgore, A., Lampinen, M., 1999. Building a California kelp database using GIS. 2000 ESRI International User Conference.
- Verdura, J., Santamaría, J., Ballesteros, E., Smale, D.A., Cefall, M.E., Golo, R., de Caralt, S., Vergés, A., Cebrian, E., 2021. Local-scale climatic refugia offer sanctuary for a habitat-forming species during a marine heatwave. J. Ecol. 109, 1758–1773.
- Wang, M., Hu, C., 2021. Satellite remote sensing of pelagic sargassum macroalgae: the power of high resolution and deep learning. Remote Sens. Environ. 264, 112631.
- Wicaksono, P., Lazuardi, W., 2018. Assessment of PlanetScope images for benthic habitat and seagrass species mapping in a complex optically shallow water environment. Int. J. Remote Sens. 39, 5739–5765.
- Wilson, K.L., Tittensor, D.P., Worm, B., Lotze, H.K., 2020. Incorporating climate change adaptation into marine protected area planning, Glob. Chang, Biol. 26, 3251–3267.
- Wulder, M.A., Masek, J.G., Cohen, W.B., Loveland, T.R., Woodcock, C.E., 2012. Opening the archive: how free data has enabled the science and monitoring promise of Landsat. Remote Sens. Environ. 122, 2–10.
- Xu, Y., Vaughn, N.R., Knapp, D.E., Martin, R.E., Balzotti, C., Li, J., Foo, S.A., Asner, G.P., 2020. Coral bleaching detection in the Hawaiian Islands using spatio-temporal standardized bottom reflectance and planet dove satellites. Remote Sens. 12, 3219.
- Yamano, H., Sakuma, A., Harii, S., 2020. Coral-spawn slicks: reflectance spectra and detection using optical satellite data. Remote Sens. Environ. 251, 112058.
- Zeng, L., Wardlow, B.D., Xiang, D., Hu, S., Li, D., 2020. A review of vegetation phenological metrics extraction using time-series, multispectral satellite data. Remote Sens. Environ. 237, 111511.